Characterization of the instrument temperature dependence of Brewer total ozone column measurements

Alberto Berjón[1,2], Alberto Redondas[3,2], Meelis-Mait Sildoja[4], Saulius Nevas[4], Keith Wilson[5], Sergio F. León-Luis[3,2], Omar el Gawhary[6], and Ilias Fountoulakis[7]

[1]University of La Laguna, Department of Industrial Engineering, S.C. de Tenerife, Spain
[2]Regional Brewer Calibration Center for Europe, Izaña Atmospheric Research Center, Tenerife, Spain
[3]Agencia Estatal de Meteorología, Izaña Atmospheric Research Center, Spain
[4]Physikalisch-Technische Bundesanstalt (PTB), Braunschweig, Germany
[5]Kipp & Zonen BV, Delft, Netherlands
[6]Dutch Metrology Institute, Delft, Netherlands
[7]Aristotle University of Thessaloniki, Laboratory of Atmospheric Physics, Thessaloniki, Greece

Correspondence to: Alberto Redondas (aredondasm@aemet.es)

Abstract. The instrumental temperature correction to be applied to the ozone measurements by the Brewer spectrophotometers is derived from measurements of the irradiance from an internal halogen lamp in the instrument. These characterisations of the Brewer instruments can be carried out within a thermal chamber, varying the temperature from -5$^{\circ}C$ to +45$^{\circ}C$, or during field measurements, making use of the natural change in ambient temperature. However, the internal light source used to determine the thermal sensitivity of the instrument could be affected in both methods by the temperature variations as well, which may affect the determination of the temperature coefficients. In order to validate the standard procedures for determining Brewer's temperature coefficients, two independent experiments using both external light sources and the internal lamps have been performed within the ATMOZ Project. The results clearly show that the traditional methodology based on the internal lamps is not affected by possible temperature effects on the internal lamps. The three methodologies yielded equivalents results, with differences in total ozone column below 0.08% for a mean diurnal temperature variation of 10$^{\circ}C$.

1 Introduction

The Brewer spectrophotometer has been used for decades as a reference instrument to retrieve total ozone column (TOC) and for validation of satellite-based measurements. TOC is retrieved from direct sun measurements at four wavelengths in the ultraviolet (UV), from 310.1 nm to 320.1 nm. In order to perform this type of measurements, this equipment operates outdoor and therefore it is exposed to environmental changes. Moreover, this instrument operates in all ~~climates~~ climatic and weather conditions, from subtropical deserts to polar zones. This exposure to weather makes it necessary to develop a mechanism that prevents the measurement results from being affected by changes in ambient temperature.

The spectrophotometer consists of a temperature-compensated monochromator that allows accurate measurements in the UV range (McElroy, 2014). Due to temperature changes the monochromator expands or contracts, which produces changes in the measured spectrum. To avoid this effect, the material of the push rod that controls the movement of the diffraction

grating is selected so that its contraction and expansion causes the opposite effect on the spectrum, thus minimizing the effect of the temperature on the measurements. ~~Furthermore,~~ Nevertheless, mechanical tolerances in the manufacturing may cause imperfections in this temperature compensation. Thus the Brewer operational procedure recommends to perform an internal Hg-lamp test (HG test) when the internal temperature varies more than $3°C$ (Environment Canada, 2008). The HG test uses a mercury discharge lamp ~~to precisely locate the~~ (line 302.15 ~~/~~nm or 296.73 nm~~mercury line~~) to check the stability of the wavelength calibration during Brewer operations. During the test, the diffraction grating is positioned such that the operating wavelengths are dispersed onto the appropriate exit slits. ~~Nevertheless, depending on the mechanical tolerances in the manufacturing, the temperature compensation may not be perfect (Gröbner et al., 1998).~~ Moreover, other elements in the spectrophotometer, such as the photomultiplier tube, can also be affected by temperature changes and, therefore, in order to ensure the accuracy of the measurements, it is necessary to characterize the thermal sensitivity of the spectrophotometer in order to correct its effect.

The Brewer spectrophotometer quality assurance protocol includes the thermal characterization of the instrument. This characterization is initially carried out inside a thermal chamber at Kipp & Zonen, manufacturer of the Brewer spectrophotometer, by measuring the output of an internal halogen lamp while varying the temperature of the chamber from -5$°C$ to +45$°C$ during a period of 72 hours. Temperature coefficients in a linear approxiamation are determined during this characterization for each of the channels used for the determination of TOC.

If an appreciable temperature dependence in the retrieved ozone is detected during the routine operation, the original coefficients are corrected using the in-field data of the internal halogen lamp measurements along the diurnal temperature variation. This procedure is normally applied during intercomparison campaigns (Redondas and Rodríguez-Franco, 2015). A drawback of this method is the narrower temperature range that is available for the field measurements compared with the thermal chamber method. However, the natural ambient temperature variation applies to the instrument during its normal operation mode, which generally yields acceptable temperature coefficients.

The determination of the thermal sensitivity of the instrument by means of the internal lamp, used in both described procedures, implies that the internal halogen lamp and the power supply circuit are also subjected to temperature changes and they can also exhibit some temperature sensitivity. This can potentially modify the lamp irradiance or its alignment, hampering the determination of the temperature coefficients. In addition, there are different elements involved in the direct sun measurements but not in the measurement of the internal lamp, such as the quartz window ~~, the ground-quartz diffuser~~ and the neutral density filters, which can make the results of the characterization to be ineffective when applied to the operational measurements.

While the temperature effect over the global UV measurements of the Brewer spectrophotometer has been studied by different authors, so far no validation of the temperature sensitivity of the TOC retrieved from the Brewer measurements has been reported. On this basis, the validation of the procedures for the retrieval of the temperature coefficients was included as one of the objectives of the EMRP ENV59 project "Traceability for atmospheric total column ozone" (ATMOZ).

In this work, we report on a comparative study of the temperature coefficients retrieved using the standard procedures (using the internal lamp in a thermal chamber and during field measurements) and two alternatives setups employing external lamps for thermal chamber measurements. For this purpose, we have made measurements with #185 and #233 MKIII ~~Brewers~~

Brewer spectrophotometers at PTB (Physikalisch-Technische Bundesanstalt) and at Kipp &Zonen facilities, respectively. Field data from the EUBREWNET (COST Action ES1207) database is also used (Rimmer et al., 2018).

2 Principle of measurement of the Brewer spectrophotometers

In order to understand how the temperature correction is applied to the measurements by the Brewer spectrophotometers we review in this section the basic measurement principles that are used to obtain the TOC from this instrument. A comprehensive description of the Brewer instrument and the TOC calculation from the results of the measurements can be found in Kerr et al. (1985).

TOC is the main product derived from solar direct irradiance measurements by the Brewer spectrophotometers. The direct irradiance measurement is performed by pointing the direct entrance port normally to the sun based on an an azimuth tracker and a rotating quartz prism which follows the sun's elevation. These measurements are made through a quartz window covering the direct port. To select the different wavelengths used in the calculation, the Brewer spectrophotometer maintains a fixed position of the diffraction grating and uses a rotating slit mask to select successively each wavelength. The rapid movement of the slit mask assures that all wavelengths are measured almost simultaneously. TOC, in Dobson units (DU) or milli-atm-cm, is ~~obtaining~~ obtained from Equation 1 (following manufacturer's nomenclature):

$$TOC = \frac{R_6 - ETC - B}{A\mu} \tag{1}$$

where R_6 is usually defined on the basis of double ratios between intensity measurements, $I_c(\lambda_i)$, at certain wavelengths (Kipp & Zonen, 2008), but can be alternatively defined as the linear combination of the common logarithm of the intensity:

$$R_6 = \sum_{i=1}^{4} \omega_i F_c(\lambda_i) \tag{2}$$

$$F_c(\lambda_i) = 10^4 log(I_c(\lambda_i)) \tag{3}$$

The coefficients, ω_i, take values of -1.0, 0.5, 2.2 and -1.7 for the wavelength of 310.1 nm, 313.5 nm, 316.8 nm and 320.1 nm respectively. These wavelengths correspond to slits 3 to 6 in the rotating slit mask of the monochromator. $I_c(\lambda_i)$ are obtained from the Brewer raw intensity after dark count, dead time, temperature and filter transmittance corrections. The wavelengths, λ_i, and coefficients, ω_i, used in Equations 2 and 3 have been especially selected to suppress the aerosol and SO_2 effects in the measured signal (Dobson, 1957; Kerr et al., 1981). In general any linear effects with wavelength is suppressed, as λ_i and ω_i

verify Equations 4 and 5. This also allows to minimize any small shift in wavelength and the influence of sulfur dioxide on the ozone retrieval (Fioletov et al., 2005).

$$\sum_{i=1}^{4} \omega_i = 0 \tag{4}$$

$$\sum_{i=1}^{4} \omega_i \lambda_i \approx 0 \tag{5}$$

ETC is a linear combination (Equation 6) of the extraterrestrial constant of the instrument, $F_{ext}(\lambda_i)$, which can be obtained from a comparison with a calibrated instrument or from the Langley plot method (Redondas, 2007).

$$ETC = \sum_{i=1}^{4} \omega_i F_{ext}(\lambda_i) \tag{6}$$

B is a linear combination of the Rayleigh transmittance of the air, $\beta(\lambda_i)$, corrected by the Rayleigh air mass, ν, and the ratio between the pressure at the observation position, p, and the standard pressure at sea level, p_0.

$$B = \nu \frac{p}{p_0} \sum_{i=1}^{4} \omega_i \beta(\lambda_i) \tag{7}$$

A is a linear combination of the ozone absorption coefficients, $\alpha(\lambda_i)$.

$$A = \sum_{i=1}^{4} \omega_i \alpha(\lambda_i) \tag{8}$$

Both the Rayleigh air mass, ν, and the ozone air mass, μ, are calculated assuming an effective altitude of 5 km and 22 km respectively (Bernhard et al., 2005).

R_6 is derived from the intensity ratios, or equivalently from Equation 2, and therefore it has no units, just like ETC and B.

3 Temperature ~~Correction~~correction

Most ~~of the light detectors~~ photo-detectors have some sensitivity to temperature. If the sensitivity can be linearly approximated, the intensity I $[c/s]$ measured at different temperatures T $[°C]$, while the detector is illuminated with a stable light source, can be expressed as:

$$I_{=} I_c - \tau_0 (T - T_0) \tag{9}$$

,

where T_0 is the reference temperature, I_c is the intensity of the source measured at the reference temperature, and τ_0 is the variation rate of the intensity with the temperature $[c/s^{\circ}C]$. We can rewrite this expression as:

$$I_c = \frac{I}{1 - \tau(T - T_0)} \tag{10}$$

where $\tau = \tau_0/Ic$ is the temperature coefficient having units of $1/^{\circ}C$. This last expression has an advantage that, while τ_0 depends on the intensity of the light source, τ is independent and we can use it to determine the intensity of the source at the reference temperature. This process is generally referred to as temperature correction.

The temperature coefficient is usually determined in a laboratory measuring a stable light source while the detector temperature is varied. τ is calculated from the linear regression between measured intensity and the temperature. From the previous equation and applying the natural logarithm, we can write:

$$ln(I_c) = ln(I) - ln(1 - \tau(T - T_0)) \tag{11}$$

For Brewer Spectrophotometers $\tau \approx 10^{-3}\ ^{\circ}C^{-1}$, then $\tau_0(T - T_0) \ll 1$ and we can approximate the natural logarithm $ln(1 + x)$ to the first order term of its Taylor expansion:

$$ln(I_c) = ln(I) + \tau(T - T_0) \tag{12}$$

In the Brewer data processing, this expression is multiplied by 10^4, the natural logarithm is replaced by common logarithm and T_0 is set to $0^{\circ}C$.

$$10^4 log(I_c) = 10^4 log(I) + \tau_b T \tag{13}$$

Where $\tau_b = 10^4 log(e)\tau$ is the Brewer temperature coefficient. Using Equation 3 we can rewrite this expressed as:

$$F_c = F + \tau_b T \tag{14}$$

We can define a Brewer relative temperature coefficient, $\tau'_b(\lambda_i)$, by subtracting the reference coefficient from coefficients derived for other spectral channels. Usually the reference coefficient is the one corresponding to the wavelength $\lambda_0 = 303.2nm$. In terms of the Brewer temperature coefficient we can express the relative coefficient as:

$$\tau'_b(\lambda_i) = \tau_b(\lambda_i) - \tau_b(\lambda_0) \tag{15}$$

Since the weights used in the common Brewer algorithm to calculate ozone are chosen to verify Equation 4, we can write the Equation 2 as:

$$R_6 = \sum_{i=1}^{4} \omega_i F_c(\lambda_i) = \sum_{i=1}^{4} \omega_i F(\lambda_i) + T \sum_{i=1}^{4} \omega_i \tau_b(\lambda_i) = \sum_{i=1}^{4} \omega_i F(\lambda_i) + T \sum_{i=1}^{4} \omega_i \tau'_b(\lambda_i) \tag{16}$$

Equation 16 shows that we can use interchangeably $\tau_b(\lambda_i)$ or $\tau'_b(\lambda_i)$ to calculate R_6 and therefor TOC.

The relative temperature coefficients, $\tau'_b(\lambda_i)$, can be calculated from Equation 15, but it can also be experimentally retrieved by the linear regression between the ratio of intensities, expressed as $F(\lambda_i) - F(\lambda_0)$, and the temperature:

$$\begin{aligned} F(\lambda_i) &= F_c(\lambda_i) - \tau_b(\lambda_i) T \\ F(\lambda_i) - F(\lambda_0) &= F_c(\lambda_i) - F_c(\lambda_0) - (\tau_b(\lambda_i) - \tau_b(\lambda_0)) T \\ F(\lambda_i) - F(\lambda_0) &= F_c(\lambda_i) - F_c(\lambda_0) - \tau'_b(\lambda_i) T \end{aligned} \tag{17}$$

The relative coefficients have the advantage that they can be reliably derived even if the illumination condition is not stable. The only requirement for the determination of the relative coefficients is that the change of the light source is proportional at all wavelengths.

Furthermore, from the previous Equations we can see that the temperature effect over R_6 can be reduced to the lineal combination of the temperature coefficients, τ_{R6}.

$$\tau_{R6} = \sum_{i=1}^{4} \omega_i \tau_b(\lambda_i) \tag{18}$$

Where $\tau_b(\lambda_i)$ can refer indistinctly to the Brewer temperature coefficients or to the relative temperature coefficients.

As discussed earlier, the temperature changes may affect the Brewer's monochromator by slightly modifying the wavelength of the measurement.

$$\begin{aligned} F(\lambda_i + \Delta\lambda) &= F(\lambda_i) + \Delta\lambda \left.\frac{\partial F}{\partial \lambda}\right|_{\lambda=\lambda_i} \\ R_6 &= \sum_{i=1}^{4} \omega_i F(\lambda_i + \Delta\lambda) = \sum_{i=1}^{4} \omega_i F(\lambda_i) + \sum_{i=1}^{4} \omega_i \Delta\lambda \left.\frac{\partial F}{\partial \lambda}\right|_{\lambda=\lambda_i} \end{aligned} \tag{19}$$

From Equation 19 we can see that the variation of R_6 will depend on how different is the derivative of the irradiance between the selected wavelengths. This effect is minimized by selecting the wavelengths at stationary points in the solar spectrum (Brewer, 1973) where $\partial F/\partial\lambda \sim 0$. In the case of the lamps used to characterize the temperature sensitivity, the spectrum is smooth enough to consider $\partial F/\partial\lambda = Cte$ in a short wavelength interval. This has the same effect and the second term of the right-hand side of the Equation 19 is cancelled as $\Delta\lambda$ is constant or proportional to λ.

4 Operating temperature

The standard operating ambient temperature range provided by the manufacturer of the Brewer spectrophotometer is from $0°C$ to +40°C. This limitation comes from the operating temperature range of the photomultiplier tube (PMT), from $0°C$ to +50°C. As the heat dissipated by the internal electronics increases the temperature in the instrument by about 5°C, the operating temperature range of the Brewer has a safety margin of 5°C.

In the case that the ambient temperature drops below $0°C$ the equipment should be operated using an internal heater that allows to extend the operating ambient temperature range to -20°C - +40°C. In practice, the internal heater is activated when instrument temperature drops below $10°C$ or $20°C$ depending of the instrument configuration. Additionally, a cold-weather cover is furnished by the manufacturer for extreme weather conditions, which allows operating the instrument at ambient temperatures as low as -50°C.

From the EUBREWNET database (http://rbcce.aemet.es/eubrewnet) we have studied the Brewer spectrophotometer internal temperatures at which the ozone measurements have been made in 32 measurement stations from 1996 to 2017. The temperature inside the instrument is registered for each ozone measurement by a sensor located next to the PMT. For this analysis, 4.2 million recorded temperatures were used. The stations involved in the study are mainly in Europe, but there are also data from Greenland, Australia, Uruguay and Algeria. They are, therefore, a very representative sample of the different environmental conditions under which the Brewer spectrophotometers are measuring throughout the world. Figure 1 shows a boxplot for all the stations. The median temperature values for all the stations are between $16°C$ and $32°C$, while the 1st and 3rd quartiles are always above $11°C$ and below $39°C$ respectively. The mean diurnal temperature variation is $12°C$. Figure 2 shows a histogram with data from all stations together. Considering all the data, the mean temperature value is $23.0°C$ and a median value is $22°C$, with a standard deviation of $16.6°C$. The 1 and 99 percentiles are estimated to correspond to $5°C$ and $44°C$. Only a small number of measurements (0.04%) are outside the safety limits for the PMT that we discussed earlier ($0°C$, $50°C$).

We have also analyzed the thermal sensitivity, τ_{R6}, of 44 Brewer spectrophotometers at the EUBRENET database, Figure 3. These values range from -0.9°C^{-1} to 4.0°C^{-1}. Two different distribution clearly appears related to the different Brewer models. MKIII model has a mean τ_{R6} value of 0.20°C^{-1} and a standard deviation of 0.52°C^{-1}. But in the case of MKII and MKIV the mean value rises to 1.54°C^{-1} and the standard deviation is 0.70°C^{-1}. While Brewer MKIII has a double monochromator to assure a low stray light influence in UV, MKII and MKIV have a single monochromator, so that they use a $NiSO_4$ filter in front of the PMT to eliminate the effect of visible light on the measurements, i.e., to reduce the stray light in the UV range. The higher temperature dependence observed in the single-monochromator Brewers is commonly attributed to this $NiSO_4$ filter (Fountoulakis et al., 2017; Cappellani and Kochler, 2000).

5 Experimental setups

To study the temperature sensitivity of Brewer spectrophotometers by using external lamps, two different experimental setups have been used: a first one at PTB in Braunschweig, Germany and a second at Kipp & Zonen in Delft, Netherlands (both shown in Figure 4). For ~~this~~ these studies, MKIII Brewers #185 and #233 were chosen. These instruments are the traveling

master istrument of the RBCC-E triad at the Izaña observatory of the Spanish National Meteorological Agency (AEMET) and a ~~reference~~ research instrument of Kipp & Zonen, respectively.

During the experiments the internal heater was turned off, but the air circulation fan was left on to evenly distribute the air inside the Brewer, allowing a uniform heating up and cooling down of the internal components.

For the Brewer #185 characterization, a dedicated climate chamber at PTB was used to provide the necessary conditions. The schematic of the measurement system is presented in Figure 5 (left). The temperature and humidity of the chamber was monitored using the built-in sensors of the chamber and two extra sensors, one PT-100 thermometer and one Almemo humidity and temperature sensor. A Hamamatsu model LC8 UV source with a built-in Xe lamp and equipped with a quartz fiber bundle as a light guide was used to illuminate simultaneously both global and direct input ports of the Brewer. The light guide was terminated with light-shaping-diffuser (LSD) to provide uniform illumination. To monitor the output stability of the UV source, a set of monitor detectors were placed close to the Brewer input ports. Those included two SiC photodiodes and a calibrated spectrometer. One of the SiC photodiodes was located inside the chamber and the other one outside. To direct the UV-radiation onto the external SiC diode a similar light guide was used as for the Xe lamp system. For optimal irradiation conditions the internal SiC photodiode and the entrance optics of the spectrometer included special quartz-based Primusil diffusers. For the external SiC photodiode, no diffuser was used to compare the readings with the diffuser-covered detectors and register any possible change of the diffuser transmittance due to the change of temperature or relative humidity in the chamber during the experiment. The Brewer observations consisted of alternately measuring the internal and the external lamps. The external Xe lamp was continuously on during the whole cycle of the characterisations while the internal lamp was turned on and off for each measurement. The drift of the Xe source irradiance at the Brewer entrance port was corrected by using the calculated mean of the normalized integrated spectral data from the monitor spectroradiometer and the temperature-corrected SiC detector readings.

The experiment was done twice at the PTB facilities. On the first occasion in January 2016, refered in the results as PTB1, the quartz fiber bundle was used to illuminate simultaneously both global and direct input ports of the Brewer. The temperature of the climate chamber was varied between -5$°C$ to +40$°C$ over a 70 hours period. Separate cycles were used above and below 0$°C$ to achieve better control over temperature and humidity. Due to some inconsistencies in the retrieved results of the first experiment, the temperature characterisations were repeated at the PTB facilities in ~~March~~ February 2017. On this second occasion, refered to as PTB2, the external lamp was aligned with the direct entrance port. The global port was not used for the measurements. In addition, the internal lamp was replaced since anomalous behavior was observed during its operation at the time of the first measurements in January 2016 and later also at the RBCC-E. Two different temperatures cycles were used at different temperature change rate. First, the temperature of the climate chamber was varied between 8$°C$ and 45$°C$ over a 64 hours period with a temperature change rate of 1.2$°C/h$. A second cycle was done varying the temperature from -8$°C$ to 30$°C$ over 50 hours with a temperature change rate of 2.8$°C/h$.

The experimental set up for characterizing Brewer #233 is shown in Figure 5 (right). The temperature in the chamber was varied from -5 to +45 during a period of 72 hours. A Laser Driven Light Source (LDLS) Energetiq EQ-99, from Dutch Metrology Institute (VSL), was used as an external lamp. By means of an optical fibre bundle, the light was guided into the

chamber, collimated by a 25 mm lens and then illuminated the Brewer's quartz window at normal incidence. The collimated beam illuminated the rotating prism, which was aligned in accordance with the incoming light. During the external lamp measurements, no lamp monitor was used, as one of the main characteristics of the LDLS is its high stability (Islam et al., 2013). The other components in the beam delivery part were assumed to be stable and independent of temperature. Two separated experiments were performed using the internal lamp in the first case and the external LDLS via the quartz window in the second case. The respectively lamps were continuously turned on during each experiments.

In all cases, each measurement cycle included an HG test, repositioning the micrometer of the diffraction grating to locate the 302.15nm line of the mercury discharge lamp.

Since different instruments have been used in each experiment (#185 at PTB and #233 at K&Z) the differences in results may be due not only to the differences of the experiment setup, but also to the different Brewer instrument.

In this work we also include an analysis of the measurements based on the internal lamps during field measurements at dates close to the characterizations in the temperature chambers.

6 Results

Results from the experiments carried out at the PTB and at Kipp & Zonen, as well as the analysis of field measurements, are presented in this section.

In Figure 6 we show results of the Brewer measurements of both the external and the internal lamp at different temperatures. For the sake of brevity, only the data for 310.1 nm wavelength are shown. The measurements at the other wavelengths show a very similar behavior. The first evident thing apparent in the figures is the difficulty of assuming a linear behavior in these measurements. Despite using different experimental setups and instruments, the results are not as expected. Only the relation between the measurement results of the internal lamp and the temperature in the K&Z experiment can be considered linear. Nevertheless, some behaviors are repeated in the two experiments at the PTB, which makes us assume that they are probably due to real changes in the behavior of lamps, detectors or the different mechanical elements during the experiments. One of this clearly observed behaviors is the presence of hysteresis cycles. This is possibly related to an inhomogeneous temperature distribution within the instrument. In any case, it is difficult to extract information from the data presented in this way.

As stated in ~~the~~ section 3, relative coefficients are intended to be more robust against variations of the experimental conditions. Figures 7, 8 and 9 show results of the relative analysis of the measurements presented versus temperature and the relative temperature coefficients derived from both the external and the internal lamps in the three experiments. The analysis of the internal lamp data from field measurements is also presented. Since the number of measurements for certain temperatures is much higher than for others, the linear regression has been performed with respect to the average values at each temperature. We can clearly see the improvement when using the relative analysis.

The analysis of the internal lamp measurements in PTB1 shows a very marked nonlinear behavior when using slit 5 and 6 relative to slit 2. Due to this, only data below 30°C have been used to make the linear regression used to obtain the relative temperature coefficient. This behavior is not repeated in PTB2. This change in the behaviour must be due to the replacement of

the internal lamp between both experiments. One week before the PTB1 experiment, the internal lamp was burned out and it had to be replaced. However, this replaced lamp used in the PTB1 experiment did not show a stable behaviour also during later field measurements. Therefore, it was replaced again in March 2016. This is also the reason why we have only a few number of measurement points to make the field data analysis shown in Figure 7. This makes us to consider Brewer #185 not stable during the PTB1 experiment and, therefore, its results will not be included in the final analysis.

On the other hand, the PTB2 experiment (Figure 8) shows more consistent results. In this case, the relations between the relative measurements and the temperature are mainly linear, although some non-linearity is observed for both the internal and the external lamp measurements between 40°C and 50°C. This non-linearity for high temperatures may be explained by the photomultiplier tube behaviour at this temperatures. Figure 10 shows the dark signals for Brewers #185 and #233 measured during PTB2 and K&Z experiments. They demonstrate different behaviour in the operating temperature range. However, for temperatures between $40°C$ and $50°C$ both show an increase in the dark signals. Additionally, dark signals of #185 show two different behaviours between $40°C$ and 50°C along the whole experiment time. From the data sets of the EUBREWENET data base we can see that the most usual behavior corresponds to the one shown by #233.

The K&Z experiment gives also a linear relation between the relative data and the temperature for both the internal and the external lamp measurements, Figure 9.

From Table 1 we can see that the determined relative temperature coefficients present important differences depending on the used data set (thermal chamber measurements with internal lamp and external lamp or field measurements with internal lamp) in both PTB2 and K&Z experiments. However, when calculating τ_{R6} the differences disappear and very similar values are obtained, as shown in Figure 11.

The differences between the τ_{R6} values retrieved from the internal and the external lamps are 0.05 and 0.01 respectively in the PTB2 and K&Z experiments. Including the field data retrieval, the differences are within about 0.08 in both PTB2 and K&Z experiments. As the typical value of the numerator in Equation 1, $R_6 - ETC - B$, is about 1000 for an optical airmass of 1, the differences in τ_{R6} of 0.08 represent a 0.08% of TOC for a diurnal temperature variation of $10°C$.

Note that the uncertainty associated to the different coefficients in Table 1 correspond to the standard uncertainty of the slopes from linear regressions in Figures 7, 8, 9 and 11. τ_{R6} coefficients can be calculated from the relative coefficients in Table 1 or directly from the linear regressions in Figure 11. But to derive the associated uncertainty of τ_{R6} from the uncertainties of the relative coefficients we should assume they are not independent variables.

7 Summary and outlook

Two experiments were conducted at the PTB (January, 2016 and March, 2017) and the Kipp & Zonen (October, 2016) facilities to validate the standard methods for the determination of the temperature dependence of the Brewer MKIII measurements used to retrieve atmospheric TOC.

These experiments confirm that the characterisations performed in a thermal chamber using either the internal lamp of the Brewer instrument or an external lamp as well as those carried out with the internal lamp during field measurements lead to

small differences in the retrieved τ_{R6}. This is so even though the values of the relative coefficients are obtained using different types of lamps. The obtained results are in agreement because the algorithm used to retrieve TOC removes any linear effect with the wavelength.

However, in spite of the robustness of the TOC calculation algorithm, the first experiment performed at PTB in January 2016 with a non-stable spectrophotometer shows that it is necessary to guarantee a good performance of the Brewer instrument before carrying out the temperature sensitivity analysis. This highlights the importance of the method based on the internal lamp measurement data in the field since it presents the best way to ensure the correct functioning of the spectrophotometer throughout its operation.

While the behavior of the relative measurements are approximately linear with temperature, absolute measurements exhibit behaviors such as hysteresis that may become difficult to model. This implies that the temperature coefficients used in the determination of TOC should not be directly used to correct the Brewer temperature sensitivity in AOD or UV measurements, which should be analyzed separately (Fountoulakis et al., 2017).

The difficulty of obtaining absolute coefficients from the measurements in the thermal chamber is probably due to the way the temperature changes affects the different elements in the Brewer spectrophotometer. Thermal expansion in the fore optics affects the alignment of the system causing a proportional change in all wavelengths. The effect on the monochromator causes small changes in the wavelength. Also the temperature affects the photomultiplier causing a nonlinear response mainly at high temperatures.

The derived relative coefficients show important differences depending on the data used for their calculation. However, the calculated τ_{R6} are very much stable. The TOC differences due to the method used to calculate the temperature coefficients τ_{R6} are below 0.08% for a mean diurnal temperature variation of $10°C$.

The analysis of the EUBREWNET data shows some temperature sensitivity differences between Brewer MKIII model and the MKII and MKIV models, may be related with $NiSO_4$ filter. Therefore the conclusions of this work can not be extended to the MKII and MKIV models.

Finally, it is worth to note that temperature correction is usually applied to measurement data using a reference temperature close to the most frequent operation temperature. A reference temperature close to the mean operational temperature means that the applied temperature correction is most of the time small and thus a low accurate estimation of the temperature sensitivity will not have a high effect over the TOC retrieval. However, this is not the case with the Brewer spectrophotometer, which use a reference temperature of 0°C while the mean operation temperature is $23°C$ and a median value of $22°C$. A change of the reference temperature will reduce the TOC uncertainty associated with the uncertainty of the temperature correction.

Competing interests. The authors declare that they have no conflict of interests.

Acknowledgements. This work has been supported by the European Metrology Research Programme (EMRP) within the joint research project ENV59 "Traceability for atmospheric total column ozone" (ATMOZ). The EMRP is jointly funded by the EMRP participating countries within EURAMET and the European Union. We further acknowledge to the ~~Dutch Metrology Institute (VSL) for loaning us the laser driven light source (LDLS)~~ COST Action ES1207 for the EUBREWNET data access and the support by the Fundación General de la Universidad de La Laguna.

References

Bernhard, G., Evans, R. D., Labow, G. J., and Oltmans, S. J.: Bias in Dobson total ozone measurements at high latitudes due to approximations in calculations of ozone absorption coefficients and air mass, Journal of Geophysical Research: Atmospheres, 110, n/a–n/a, https://doi.org/10.1029/2004JD005559, http://dx.doi.org/10.1029/2004JD005559, d10305, 2005.

Brewer, A. W.: A replacement for the Dobson spectrophotometer?, Pure and Applied Geophysics, 106, 919–927, https://doi.org/10.1007/BF00881042, 1973.

Cappellani, F. and Kochler, C.: Temperature effects correction in a Brewer MKIV spectrophotometer for solar UV measurements, Journal of Geophysical Research: Atmospheres, 105, 4829–4831, https://doi.org/10.1029/1999JD900254, http://dx.doi.org/10.1029/1999JD900254, 2000.

Dobson, G. M. B.: Observers' handbook for the ozone spectrophotometer, in: Annals of the International Geophysical Year, V, pp. 46–89, Pergamon Press, 1957.

Environment Canada: Standard Operating Procedures Manual for the Brewer Spectrophotometer, Tech. rep., Environment and Climate Change Canada, http://woudc.org/resources/sop.php, 2008.

Fioletov, V. E., Kerr, J. B., McElroy, C. T., Wardle, D. I., Savastiouk, V., and Grajnar, T. S.: The Brewer reference triad, Geophysical Research Letters, 32, https://doi.org/10.1029/2005GL024244, l20805, 2005.

Fountoulakis, I., Redondas, A., Lakkala, K., Berjon, A., Bais, A. F., Doppler, L., Feister, U., Heikkila, A., Karppinen, T., Karhu, J. M., Koskela, T., Garane, K., Fragkos, K., and Savastiouk, V.: Temperature dependence of the Brewer global UV measurements, Atmospheric Measurement Techniques, 10, 4491–4505, https://doi.org/10.5194/amt-10-4491-2017, https://www.atmos-meas-tech.net/10/4491/2017/, 2017.

Gröbner, J., Wardle, D. I., McElroy, C. T., and Kerr, J. B.: Investigation of the wavelength accuracy of Brewer spectrophotometers, Appl. Opt., 37, 8352–8360, https://doi.org/10.1364/AO.37.008352, 1998.

Islam, M., Ciaffoni, L., Hancock, G., and Ritchie, G. A. D.: Demonstration of a novel laser-driven light source for broadband spectroscopy between 170 nm and 2.1 [small mu]m, Analyst, 138, 4741–4745, https://doi.org/10.1039/C3AN01020A, 2013.

Kerr, J. B., McElroy, C. T., and Olafson, R. A.: Measurements of ozone with the Brewer ozone spectrophotometer, in: Proceedings of the Quadrennial Ozone Symposium held in Boulder, Colorado, August 1980, pp. 74–79, J. London, ed., 1981.

Kerr, J. B., McElroy, C. T., Wardle, D. I., Olafson, R. A., and Evans, W. F. J.: The Automated Brewer Spectrophotometer, in: Atmospheric Ozone: Proceedings of the Quadrennial Ozone Symposium held in Halkidiki, Greece 3–7 September 1984, edited by Zerefos, C. S. and Ghazi, A., pp. 396–401, Springer Netherlands, Dordrecht, https://doi.org/10.1007/978-94-009-5313-0_80, 1985.

Kipp & Zonen: Brewer MKIII Spectrophotometer Operators Manual., Tech. rep., Kipp & Zonen Inc., http://www.kippzonen.com/Download/207/Brewer-MkIII-Operator-s-Manual, 2008.

McElroy, C. T.: Brewer Ozone Spectrophotometer Mechanical Design Principles, Izaña Atmospheric Research Center, Tenerife, Spain, http://kippzonen-brewer.com/wp-content/uploads/2014/10/BrewMechDesign1_McElroy.pdf, 14th WMO-GAW Brewer Users Group Meeting / COST Action ES1207 EUBREWNET Open Congress, 2014.

Redondas, A.: Ozone absolute Langley calibration, The Tenth Biennial WMO Consultation on Brewer Ozone and UV Spectrophotometer Operation, Calibration and Data Reporting, Edited by C. T. McElroy and E. W. Hare, Gaw Report. No. 176, WMO TD No. 1420, 12–14, 2007.

Redondas, A. and Rodríguez-Franco, J.: Ninth Intercomparison Campaign of the Regional Brewer Calibration Center Europe (RBCC-E), no. 224 in WMO/GAW Reports, World Meteorological Organization, http://www.wmo.int/pages/prog/arep/gaw/documents/Final_GAW_224.pdf, 2015.

Rimmer, J. S., Redondas, A., and Karppinen, T.: EuBrewNet – A European Brewer network (COST Action ES1207), an overview, Atmospheric Chemistry and Physics Discussions, 2018, 1–14, https://doi.org/10.5194/acp-2017-1207, https://www.atmos-chem-phys-discuss.net/acp-2017-1207/, 2018.

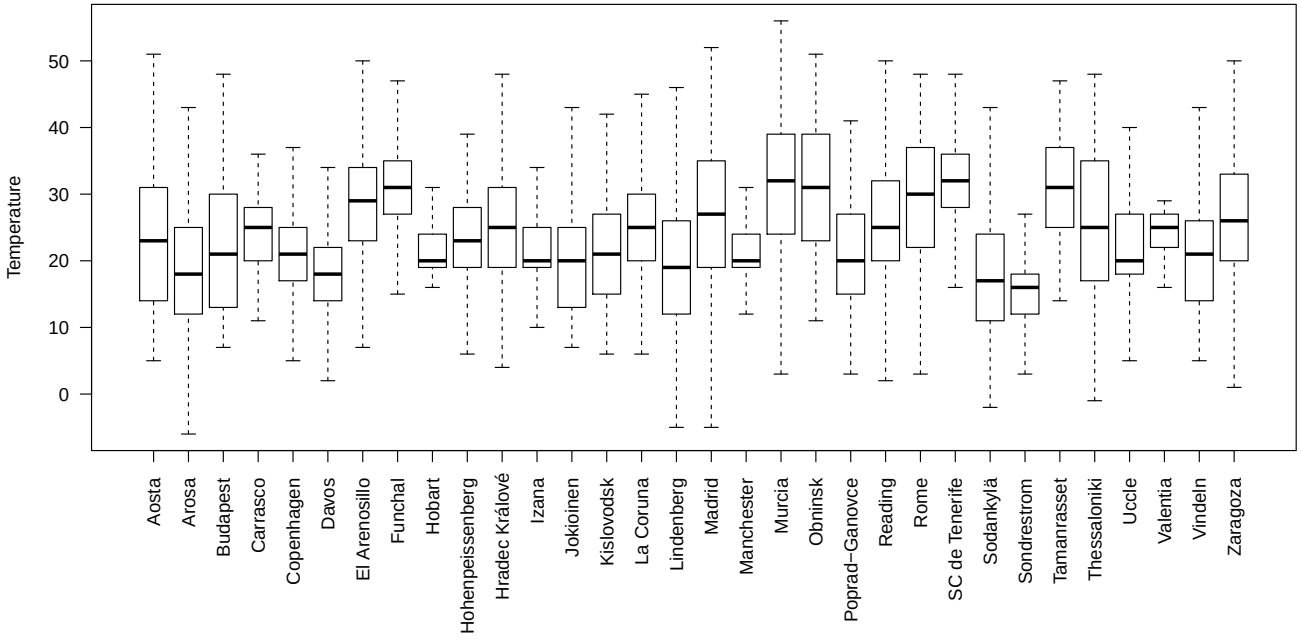

Figure 1. Statistics of each of the 32 stations used for the analysis of the operational instrumental temperatures. The 1st and 3rd quartiles are always above $11^{\circ}C$ and below $39^{\circ}C$ respectively.

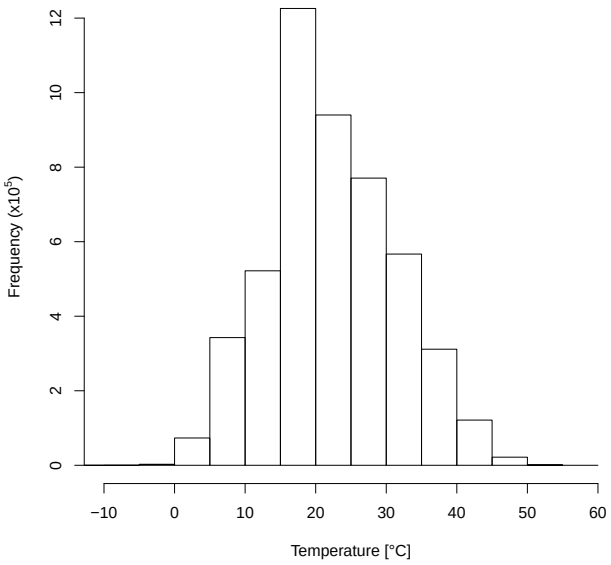

Figure 2. Frequency distribution of instrument temperatures from EUBREWNET database. 4.2 million temperature data points have been used. Only a 0.04% of measurements are outside the recommended limits ($0^{\circ}C$ and $50^{\circ}C$).

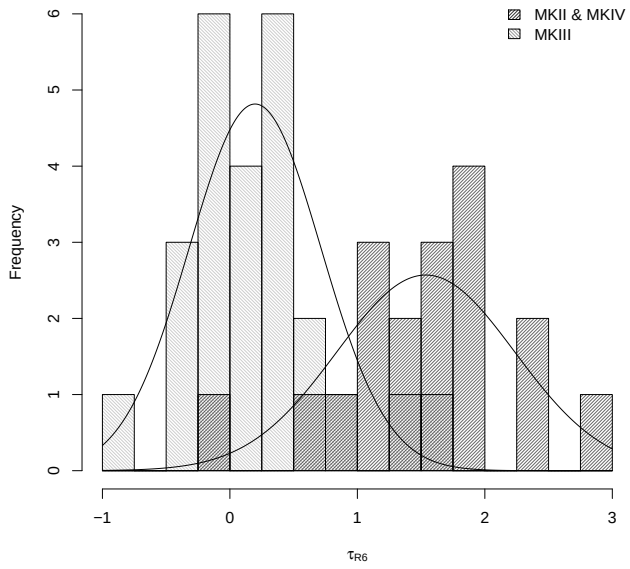

Figure 3. Temperature sensitivity of the different Brewer models.

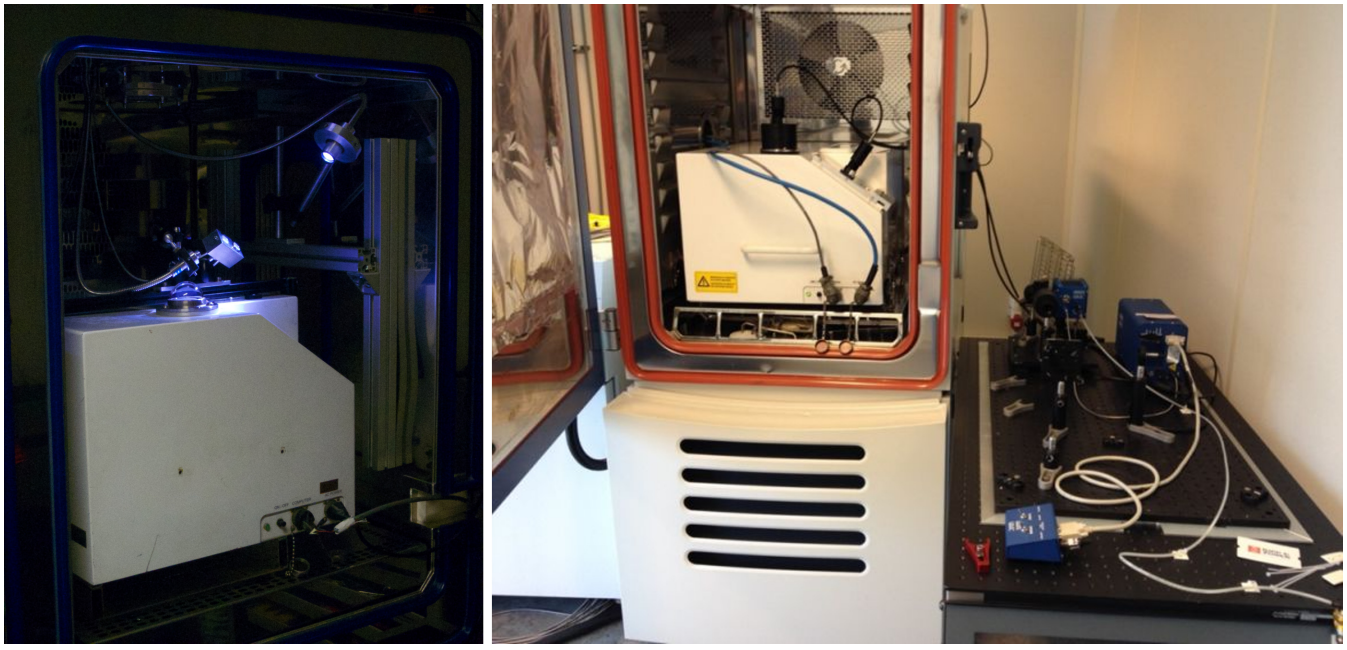

Figure 4. Pictures showing Brewer instruments in the controlled environment chambers for the measurements at the PTB (left) and at the Kipp & Zonen facilities (right).

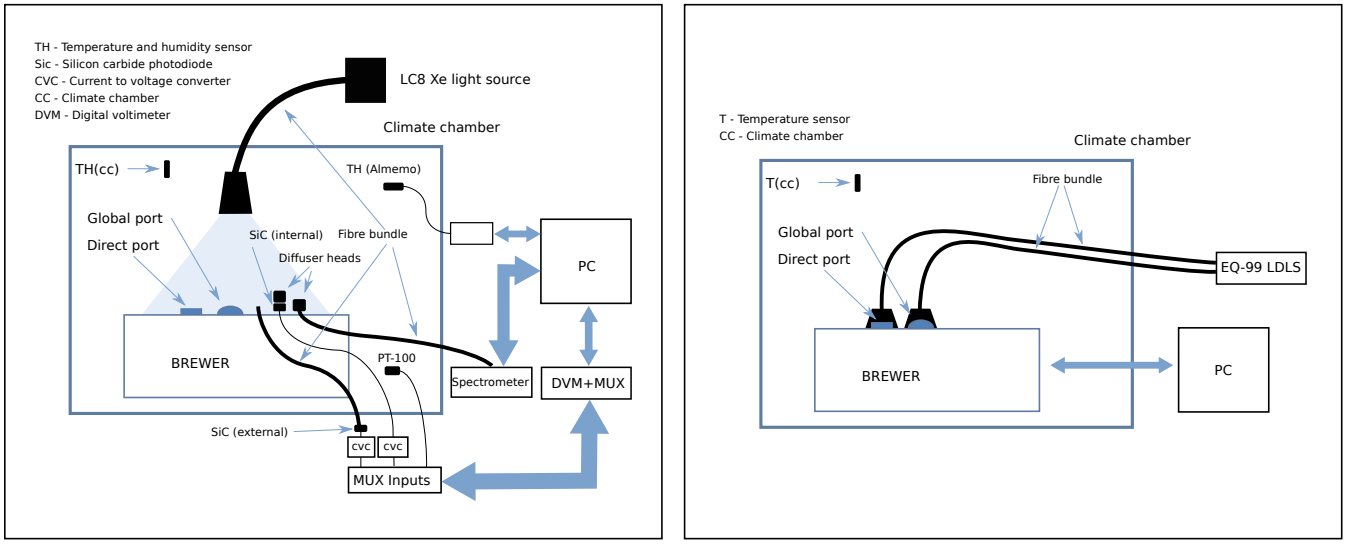

Figure 5. Measurement setups for used for the Brewer characterizations at PTB (left) and at Kipp & Zonen (right).

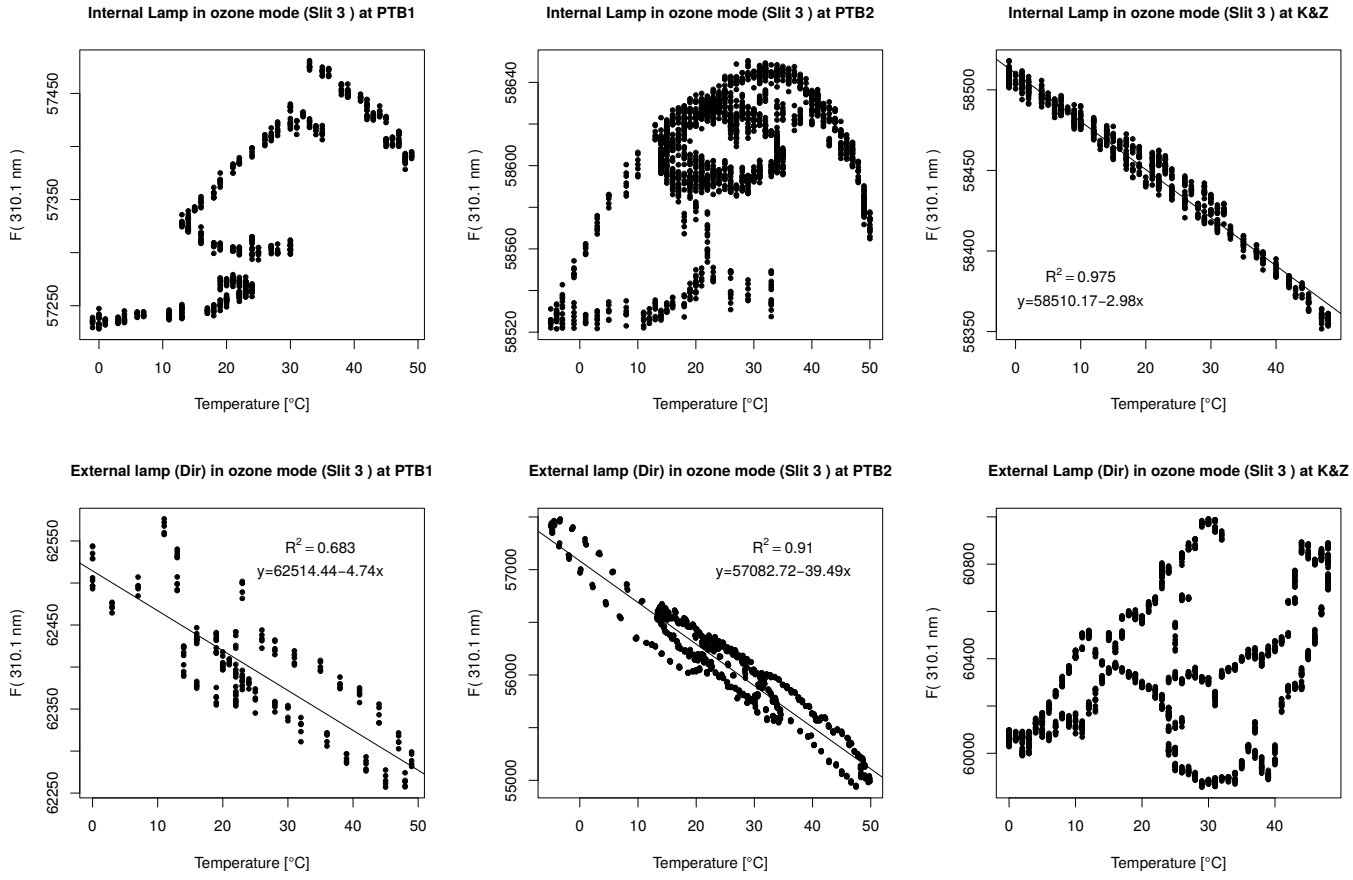

Figure 6. Scatter plot of Brewer measurement data (Slit 3) versus temperature in the temperature chambers from PTB1, PTB2 and K&Z experiments when illuminating with the internal (upper plots) and the external lamps (lower plots).

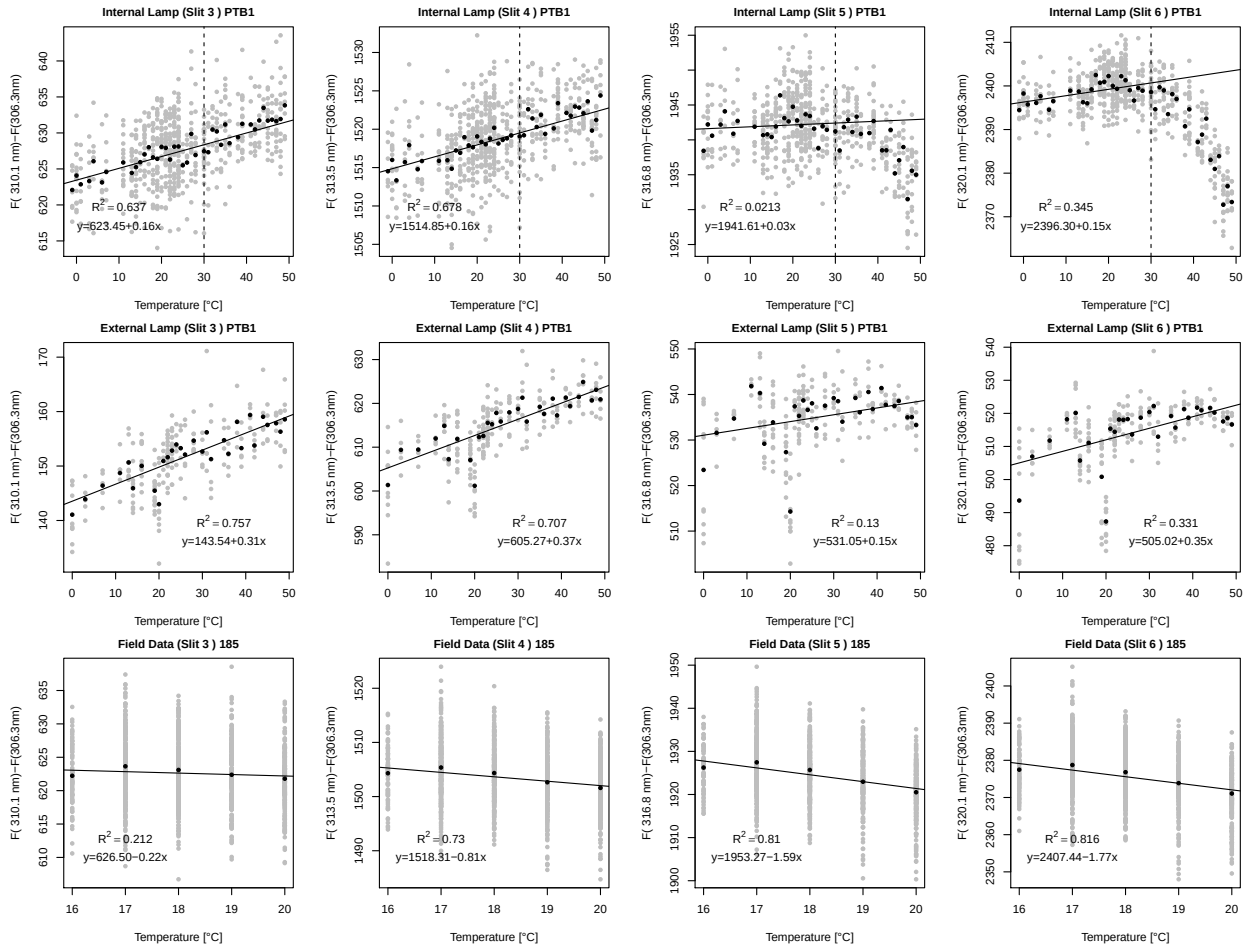

Figure 7. PTB1 experiment. Linear regression between relative Brewer data (Slit 3, 4, 5 and 6 relative to Slit 2) and temperature coefficients determined from internal and external lamp measurements in the temperature chamber and from field data. Dark points represent average values at each temperature.

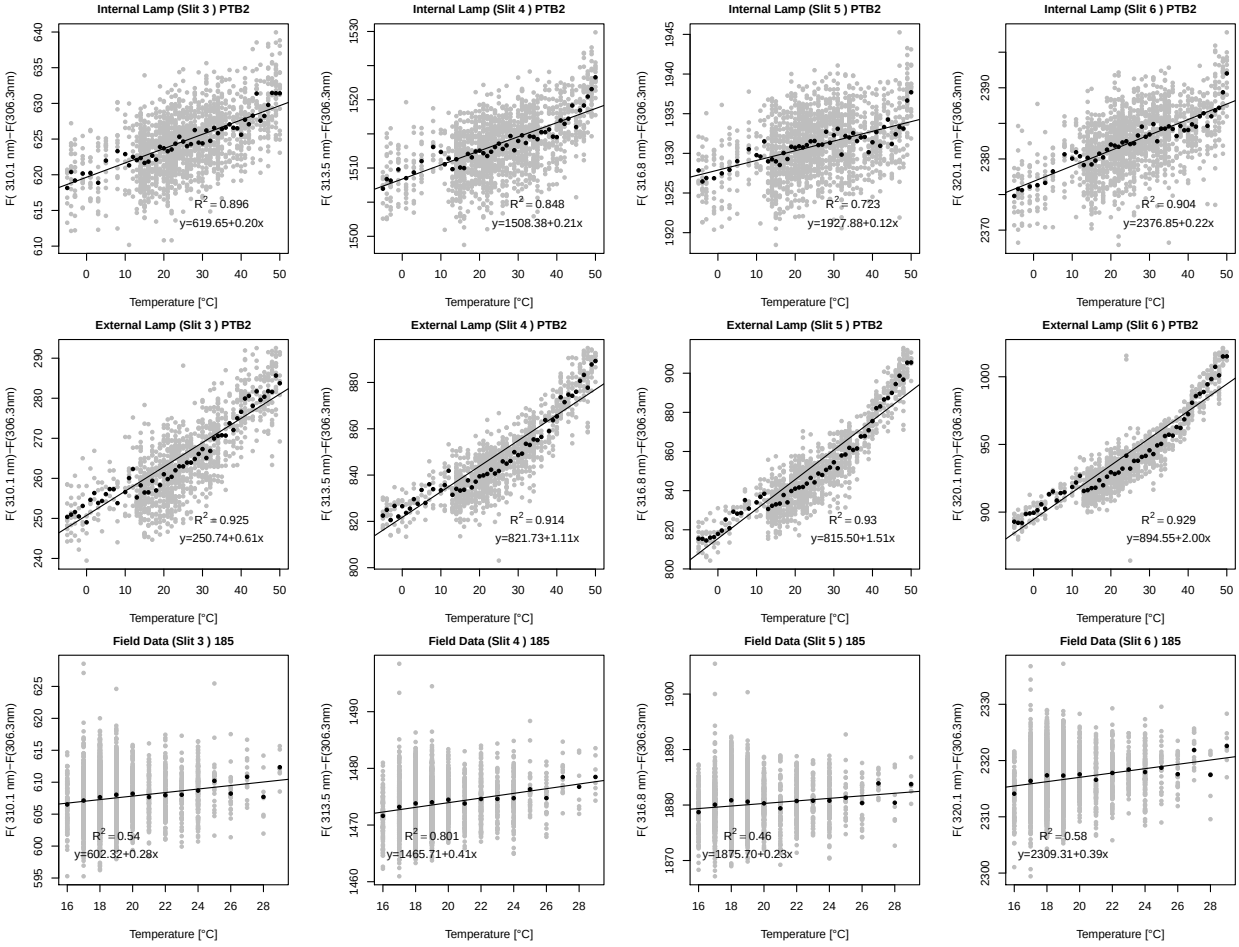

Figure 8. PTB2 experiment. Linear regression between relative Brewer data (Slit 3, 4, 5 and 6 relative to Slit 2) and temperature coefficients determined from internal and external lamp measurements in the temperature chamber and from field data. Dark points represent average values at each temperature.

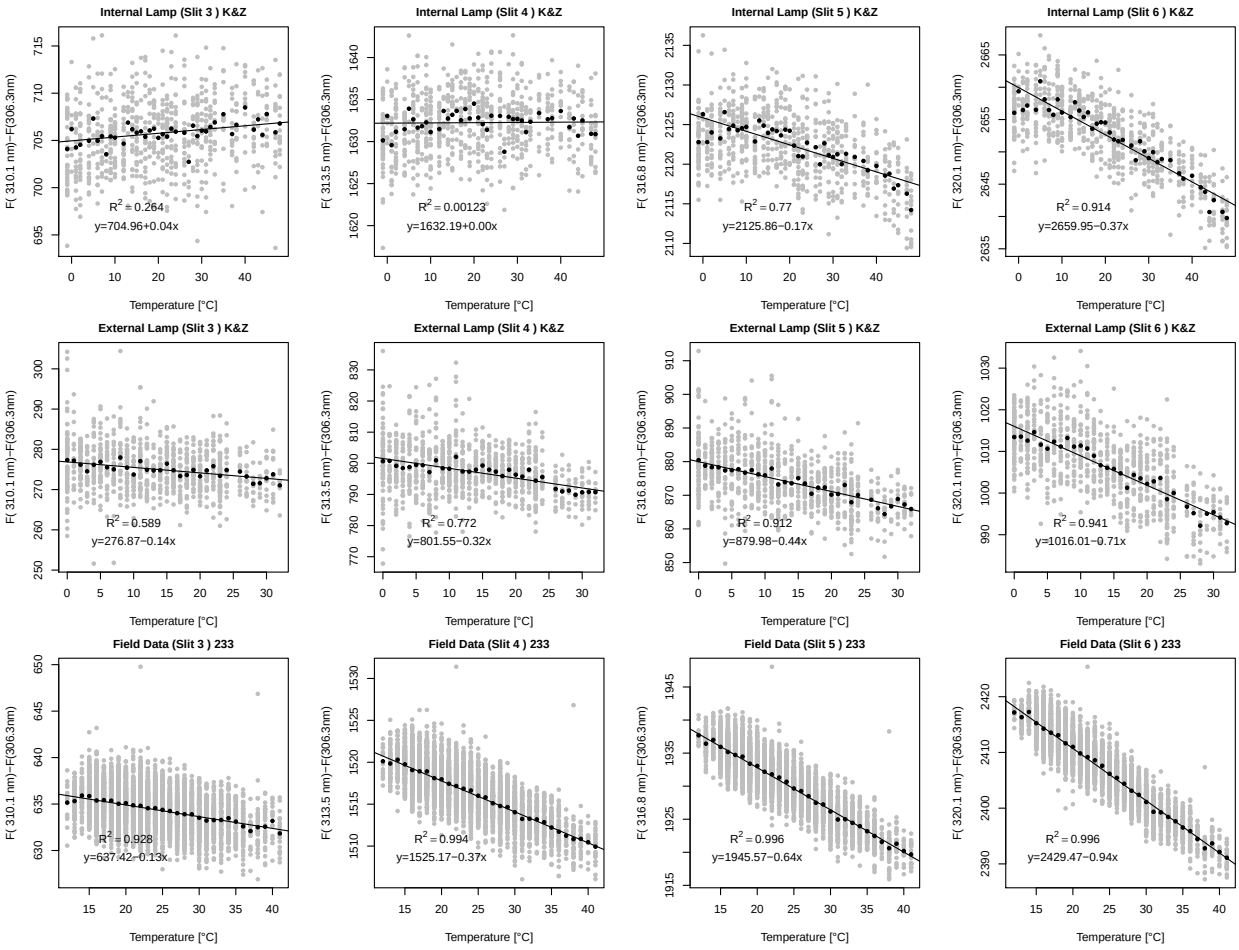

Figure 9. K&Z experiment. Linear regression between relative Brewer data (Slit 3, 4, 5 and 6 relative to Slit 2) and temperature coefficients determined from internal and external lamp measurements in the temperature chamber and from field data. Dark points represent average values at each temperature.

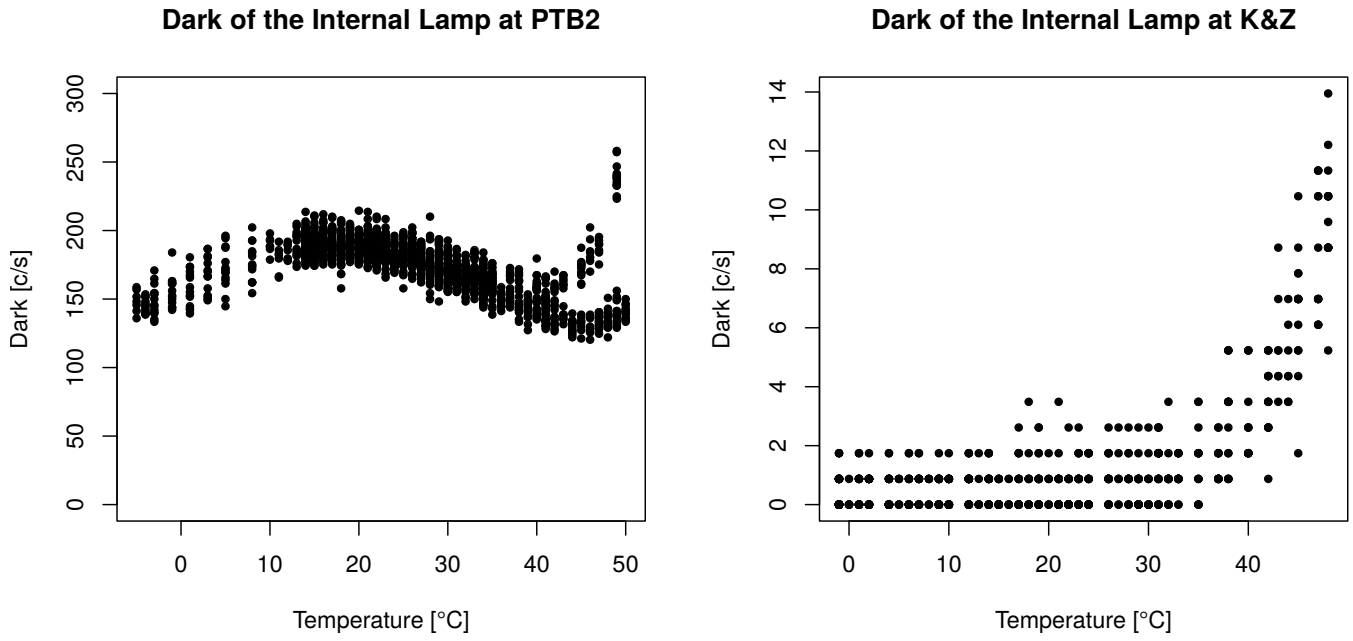

Figure 10. Dark signal values during the PTB2 and the K&Z experiments.

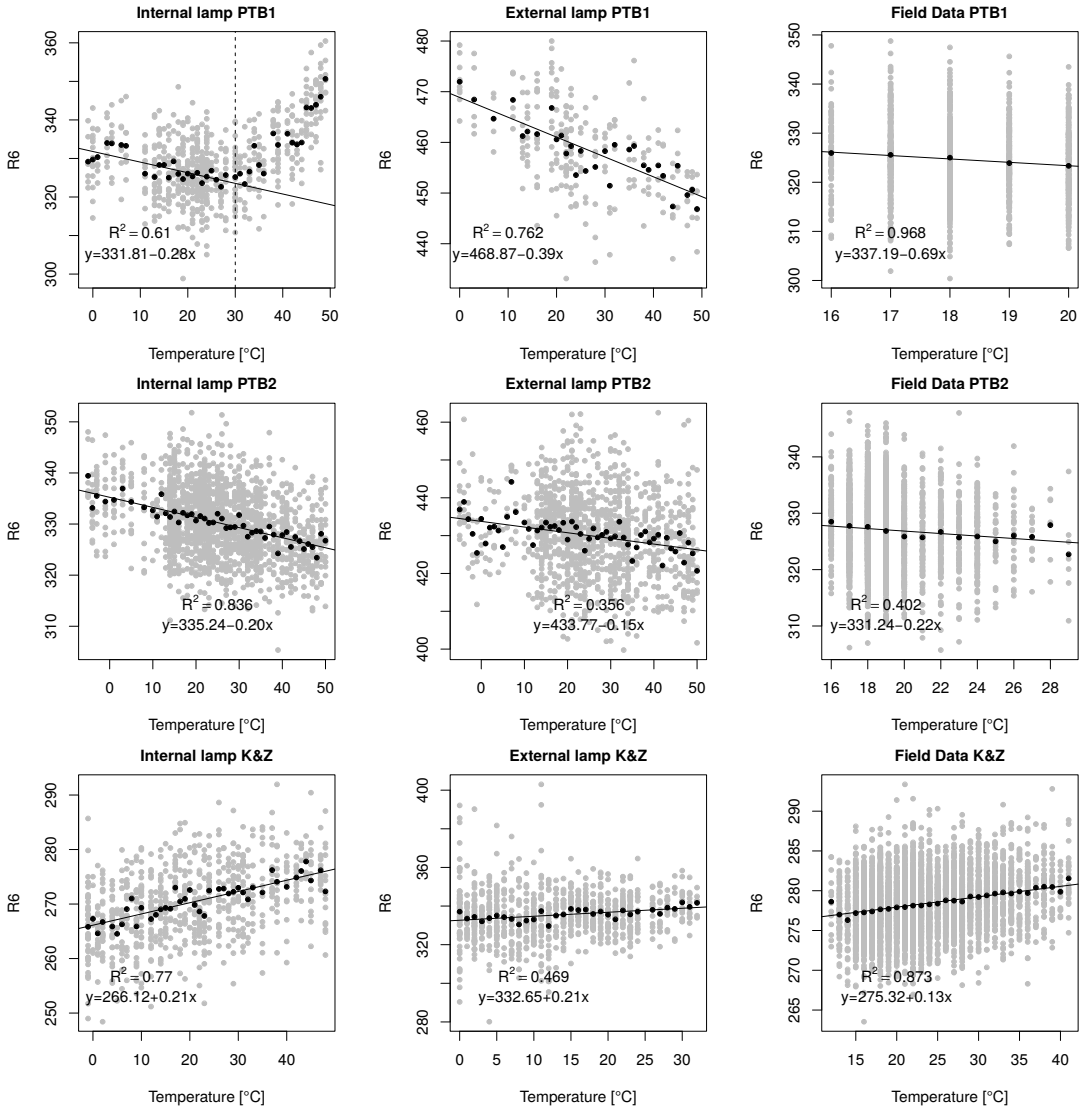

Figure 11. Linear regression between τ_{R6} and temperature for PTB1, PTB2 and K&Z experiments using internal and external lamp in the temperature test chamber and from field data. Dark points represent average values at each temperature.

Table 1. Temperature coefficients for slit 3, 4, 5 and 6 retrieved from Brewer measurements relative to slit 2 (τ_b') and temperature coefficient for R_6 (τ_{R6}). Rows are grouped in three blocks representing the tree experiments (PTB1, PTB2 and K&Z). For each experiment, results from external (top row) and internal (middle row) lamp measurements in the temperature chamber, and derived from field data (bottom row) are shown.

Experiment	$\tau_b'(310nm)$ $[^\circ C^{-1}]$	$\tau_b'(313nm)$ $[^\circ C^{-1}]$	$\tau_b'(316nm)$ $[^\circ C^{-1}]$	$\tau_b'(320nm)$ $[^\circ C^{-1}]$	τ_{R6} $[^\circ C^{-1}]$
PTB1 Ext.Lamp	-0.31 ± 0.03	-0.37 ± 0.05	-0.15 ± 0.07	-0.35 ± 0.09	0.39 ± 0.04
PTB1 Int.Lamp	-0.16 ± 0.03	-0.16 ± 0.02	-0.03 ± 0.04	-0.15 ± 0.04	0.28 ± 0.05
PTB1 Field	0.22 ± 0.24	0.81 ± 0.29	1.59 ± 0.45	1.77 ± 0.49	0.70 ± 0.07
PTB2 Ext.Lamp	-0.61 ± 0.02	-1.11 ± 0.05	-1.51 ± 0.06	-2.00 ± 0.08	0.15 ± 0.03
PTB2 Int.Lamp	-0.20 ± 0.01	-0.21 ± 0.01	-0.12 ± 0.01	-0.22 ± 0.01	0.20 ± 0.01
PTB2 Field	-0.28 ± 0.07	-0.41 ± 0.06	-0.23 ± 0.07	-0.39 ± 0.09	0.22 ± 0.08
K&Z Ext.Lamp	0.14 ± 0.02	0.32 ± 0.03	0.44 ± 0.03	0.71 ± 0.03	-0.21 ± 0.04
K&Z Int.Lamp	-0.04 ± 0.01	-0.00 ± 0.01	0.17 ± 0.01	0.37 ± 0.02	-0.21 ± 0.02
K&Z Field	0.13 ± 0.01	0.37 ± 0.01	0.64 ± 0.01	0.95 ± 0.01	-0.13 ± 0.01